



pubs.acs.org/estwater Article

Subsewershed SARS-CoV-2 Wastewater Surveillance and COVID-19 Epidemiology Using Building-Specific Occupancy and Case Data

Alasdair Cohen, Ayella Maile-Moskowitz, Christopher Grubb, Raul A. Gonzalez, Alessandro Ceci, Amanda Darling, Laura Hungerford, Ronald D. Fricker, Jr., Carla V. Finkielstein, Amy Pruden, and Peter J. Vikesland*



Cite This: https://doi.org/10.1021/acsestwater.2c00059



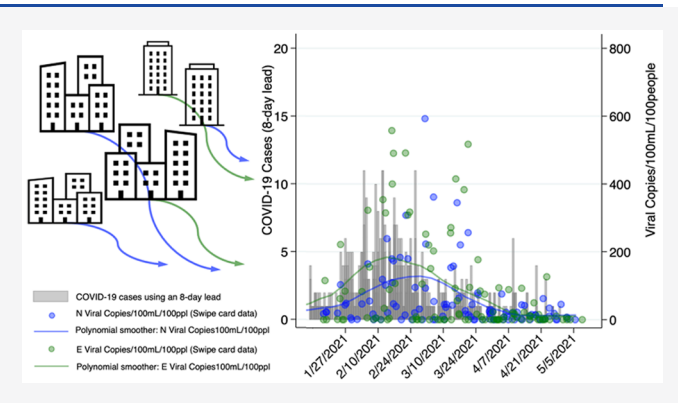
ACCESS

Metrics & More

Article Recommendations

s Supporting Information

ABSTRACT: To evaluate the use of wastewater-based surveil-lance and epidemiology to monitor and predict SARS-CoV-2 virus trends, over the 2020–2021 academic year we collected wastewater samples twice weekly from 17 manholes across Virginia Tech's main campus. We used data from external door swipe card readers and student isolation/quarantine status to estimate building-specific occupancy and COVID-19 case counts at a daily resolution. After analyzing 673 wastewater samples using reverse transcription quantitative polymerase chain reaction (RT-qPCR), we reanalyzed 329 samples from isolation and nonisolation dormitories and the campus sewage outflow using reverse transcription digital droplet polymerase chain reaction (RT-ddPCR). Population-adjusted viral copy means from isolation



dormitory wastewater were 48% and 66% higher than unadjusted viral copy means for N and E genes (1846/100 mL to 2733/100 mL/100 people and 2312/100 mL to 3828/100 mL/100 people, respectively; n = 46). Prespecified analyses with random-effects Poisson regression and dormitory/cluster-robust standard errors showed that the detection of N and E genes were associated with increases of 85% and 99% in the likelihood of COVID-19 cases 8 days later (incident—rate ratio (IRR) = 1.845, p = 0.013 and IRR = 1.994, p = 0.007, respectively; n = 215), and one-log increases in swipe card normalized viral copies (copies/100 mL/100 people) for N and E were associated with increases of 21% and 27% in the likelihood of observing COVID-19 cases 8 days following sample collection (IRR = 1.206, p < 0.001, n = 211 for N; IRR = 1.265, p < 0.001, n = 211 for E). One-log increases in swipe normalized copies were also associated with 40% and 43% increases in the likelihood of observing COVID-19 cases 5 days after sample collection (IRR = 1.403, p = 0.002, n = 212 for N; IRR = 1.426, p < 0.001, n = 212 for E). Our findings highlight the use of building-specific occupancy data and add to the evidence for the potential of wastewater-based epidemiology to predict COVID-19 trends at subsewershed scales.

KEYWORDS: wastewater-based surveillance, wastewater-based epidemiology, subsewershed, COVID-19, SARS-CoV-2, digital droplet PCR

■ INTRODUCTION

Wastewater-based surveillance (WBS) has long been used as a supplement to clinical surveillance for diseases such as polio (since the 1940s)¹ as well as for other purposes such as monitoring illicit drug use^{2,3} and supporting vaccination campaigns aimed at eradicating poliomyelitis and vaccine-derived poliovirus outbreaks.⁴ During the early stages of the current coronavirus disease 2019 (COVID-19) pandemic, it was established that SARS-CoV-2, the virus that causes COVID-19, was shed in feces.^{5,6} Subsequently, globally distributed teams adopted WBS to monitor and assess infection trends, particularly in regions with limited clinical testing.

SARS-CoV-2 may be quantified in clinical or wastewater samples through the detection of viral RNA; this requires

targeting viral genes that are unique to the virus. Early in the pandemic, national health agencies and private companies worked to develop diagnostic kits primarily using reverse transcription quantitative polymerase chain reaction (RT-qPCR). The World Health Organization (WHO) released guidelines for diagnosing COVID-19 in which they recommended nucleic acid amplification methods (e.g., RT-qPCR)

Special Issue: Wastewater Surveillance and Community Pathogen Detection

Received: January 31, 2022 Revised: April 25, 2022 Accepted: April 27, 2022



that target regions on the *N*, *E*, and *S* genes of the virus. The U.S. Centers for Disease Control and Prevention (CDC) developed its own primers targeting three regions of the nucleocapsid gene (N1, N2, N3), whereas others developed primers targeting the envelope (*E*) and spike protein (*S*) genes. RT-qPCR results yield cycle threshold (Ct) values that indicate the number of cycles needed for a sample to amplify above a specified threshold level, and these Ct values are expected to be inversely correlated with viral concentrations.

Once it was shown that viral RNA was detectable in wastewater by RT-qPCR and could be used to predict trends in clinical cases, ¹² other groups adopted WBS as a means to attempt to monitor and predict COVID-19 infection trends and outbreaks. ^{13–16} Building on this work, in mid 2020, Virginia Tech (VT), a large university that comprises the majority of the population of rural Blacksburg, VA, added wastewater surveillance to the university's COVID-19 operational plan^{17,18} with the goal of providing additional data to support campus-wide public health decision-making and the allocation of testing resources for the university's on-campus residential facilities (dormitories). Many other universities and colleges also initiated COVID-19-focused WBS programs for their campuses as well as surrounding communities.

While WBS can be used to support disease monitoring and mitigation efforts, there are many challenges associated with the use of WBS for the detection and monitoring of viruses such as SARS-CoV-2. For one, viral shedding timing and concentrations vary by pathogen, pathogen variant, and infected individual, meaning that, depending on the size of a given population and case incidence, WBS results may or may not reliably reflect infection trends. ^{22–24} Constituents that are common in wastewater may also inhibit the amplification of genes, resulting in false negatives.²³ The manner in which samples are collected also plays an important role, as does the method of analysis. ²⁵ Composite and grab sampling techniques must be considered along with heterogeneity in the volume, flow, and nature of the wastewater sampled.²⁶ With regard to extending WBS to wastewater-based epidemiology (WBE), in addition to the challenges associated with measuring and quantifying the signal in wastewater samples, sufficiently reliable and linked outcome data are needed, as are data on the size and nature of the population contributing to the wastewater being sampled. Estimation bias associated with these interrelated issues varies spatially and temporally, as well as by scale of sampling and analysis, from sewershed to subsewershed and building-specific WBS.

In the process of assisting the VT administration with the establishment of a COVID-19 WBS program that could effectively generate data to support efforts to monitor and control SARS-CoV-2 infections on campus, we identified knowledge gaps that needed to be addressed to advance the application of WBS and WBE of COVID-19 more broadly. The overarching objective of this research was to improve the understanding of the relationships between SARS-CoV-2 detected in sewage and COVID-19 case data at buildingscales, and to improve guidance on subsewershed sample collection and analysis strategies. To achieve this, we collected and analyzed wastewater samples from a cross-section of buildings across the VT campus with an emphasis on dormitories to quantify SARS-CoV-2. To extend from WBS to WBE, we coupled these data with building-specific highresolution occupancy data and student COVID-19 case status

data. With regard to specific research objectives, we sought to evaluate whether the analysis of unadjusted and population-adjusted SARS-CoV-2 viral concentrations in wastewater samples could be used to reliably predict cases of COVID-19 at building-specific scales using prespecified lead times from sample collection to case identification. We anticipate that findings from this research can be used to help improve WBS and WBE application at subsewershed scales.

METHODS

Our analyses were based on a number of data sources described in more detail in the sections that follow. Briefly, wastewater samples were collected from multiple sites/ buildings as well as the university's primary wastewater outflow twice weekly starting September 2020 through May 2021 (the VT fall 2020 semester started in August and concluded in December 2020, and the spring 2021 semester started in January and concluded in May 2021). Building occupancy estimates were derived from two data sources: swipe card data for those buildings with exterior doors operated via card readers and weekly occupancy counts from university administration. Building-specific estimated COVID-19 cases were derived from data on student-specific assignments to isolation and quarantine. University-wide COVID-19 case data were obtained from the university's health center and COVID-19 dashboard management team.

Our study was approved by VT's Institutional Review Board (#21-110). Prior to data analysis, we prepared a prespecified statistical analysis plan (uploaded to Open Science Framework).²⁷

Wastewater Sampling Sites and Protocols. With the broader goal of sampling widely across the campus, sampling sites were selected on the basis of practicality (layout and accessibility of the sewer) and with a focus on sites from which we could collect outflow from specific dormitories/buildings rather than those sampling sites with mixed wastewater flows from multiple residential and nonresidential buildings (though we did also collect samples from several multibuilding collection points). Wastewater samples were collected twice weekly (typically Mondays and Thursdays) from 17 manholes across the VT main campus in Blacksburg, VA from September 17, 2020 to May 6, 2021.

During the fall 2020 semester, grab samples were collected at all locations until composite samplers became available in October 2020. Depending on manhole access and depth as well as other logistical considerations, samples were collected as 24 h composite samples where possible and as grab samples otherwise. Composite samples were collected using either ISCO 6712 or ISCO 3700 (Teledyne Inc., Louisville, KY) automatic samplers every 30 min for 24 h (7 am to 7 am) on weekends and during the week. Some sampling dates were missed due to extreme weather, university holidays (e.g., Thanksgiving, November 21–29, 2020), and the winter break between the fall and spring semesters (December 18, 2020 to January 19, 2021). Data on selected sampling sites and methods by building and semester are summarized in Table S1.

With regard to protocols, one liter was collected from each site and stored on ice until transported to the laboratory for analysis (typically within 1.5–2 h of collection). A subset from each sample was prepared for further processing following the methods described in Ahmed et al.²⁸ Briefly, MgCl₂ was added to 150–200 mL samples for a final concentration of 25 mM,

and the pH was adjusted to 3–4. To quantify loss through filtering and extraction, bovine coronavirus (CALF-GUARD; Zoetis, Parsippany, NJ) was spiked into the samples at 1 μL of BCoV/1 mL of sample (between 1.43 \times 10 7 and 1.90 \times 10 7 copies). Following these adjustments, samples were filtered through 0.45 μm mixed cellulose ester filters (Thermofisher Scientific, Waltham, MA) using sterilized vacuum filter holders within a BSL-2 hood. Filters were then rolled and torn into 3–5 mm sized pieces using flame sterilized tweezers and then transferred into centrifuge tubes. Torn filters were stored at –80 °C until they could be transported on ice to the Molecular Diagnostics Laboratory at the VT Fralin Biomedical Research Institute where RNA extraction and RT-qPCR was performed (described below).

Extraction and PCR. To determine the viral concentrations in wastewater samples, we used two PCR approaches. Samples were labeled using coded identifiers so those conducting the RT-qPCR and reverse transcription digital droplet polymerase chain reaction (RT-ddPCR) analyses would not know from which sites the samples had been collected. Initially, we used an RT-qPCR assay developed by Ceci et al.,²⁹ who had received Emergency Use Authorization (EUA #200383) from the U.S. Food and Drug Administration (FDA). We opted to use this approach because it was FDA authorized and used for clinical testing for the VT campus (as well as for samples from Health Districts across southwest VA) and because the Molecular Diagnostics Laboratory at the VT Fralin Biomedical Research Institute had the capacity and staff to analyze wastewater samples in a timely fashion (typically providing results the same day processed samples were received).

Specimens from filter membranes were eluted in a DNA/ RNA stabilizer buffer (137 mM NaCl, 2.7 mM KCl, 8 mM Na₂HPO₄, 2 mM KH₂PO₄, 50 mM KCl, 8 mM DTT, 40 Units/mL of RNasin, pH 7.6) following a mechanical procedure to facilitate the release of particles from the membrane. An aliquot of the eluate (300 μ L) was subjected to a TRIzol/EtOH-based nucleic acid extraction protocol in a 96-well format column system (ZYMO RESEARCH) following standard extraction/washing procedures as described in Ceci et al.²⁹ Total RNA was eluted in water and quantified using a Nanodrop system (Nanodrop 200c [Thermofisher]; RNA concentrations varied from 5 to 280 ng/ μ L depending on the original sample). Five nanograms of RNA was used as template in a Power SYBR Green RNA-to CT 1-Step (Thermofisher) RT-qPCR reaction in a formulation that contains RNase inhibitor and additives to reduce the primer's secondary structure formation. Under these conditions, false positives resulting from primer dimers were less likely to occur.

Three sets of SARS-CoV-2 genes, N, E, and S, along with a housekeeping gene (hRPP30), were evaluated for amplification in independent reaction mixtures (standard curves were included in each plate and for each run, and curves were considered acceptable when R2 values were >0.98). This approach allowed for higher specificity (and helped reduce the would-be number of false negative results among clinical samples). Serial dilutions (10 000 to 10 copies per reaction) of 2019-nCoV_N_Positive control (200 000 copies/ μ L, IDT) and 2019-nCoV_N_ Hs_RPP30_Positive control (200 000 copies/ μ L, IDT) plasmids were used for each standard curve. Because the primers were designed to anneal in the 5′ and 3′ flanking regions of the target control gene, there was no need to linearize either plasmid control. Cut-off Ct and 95%

confidence interval (CI) values were experimentally determined on the basis of standard curves. The limit of detection (LoD) was 10 copies per reaction and determined as previously described. Pegative controls were used to monitor cross-contamination during RNA extraction and sample set up (no template RT-qPCR reaction for each set of primers tested in each plate). Heat-inactivated SARS-CoV-2 (ATCC cat# VR-1986HK) was used as a positive amplification control for *N*, *E*, and *S* sets of primers.

To explore the potential for improved detection sensitivity,²⁵ following analysis of the RT-qPCR results from all collected wastewater samples (described below), in November 2021, RNA extracts from sampling sites matched to dormitories for which we had relatively complete occupancy and COVID-19 case data (n = 280 samples) as well as RNA extracts from the campus outflow site samples (n = 49) were sent on dry ice to the Hampton Roads Sanitation District (HRSD), Virginia Beach, VA, for independent analysis using RT-ddPCR. For this subset of samples, a one-step RT-ddPCR multiplex was used to quantify N and E genes in the samples using no template controls, field blanks, and Twist Synthetic SARS-CoV-2 RNA Control 4 (Twist Bioscience, San Francisco, CA, USA) positive standards according to methods described in Gonzalez et al.³⁰ The LoDs, irrespective of sample volume, were 2.2 and 16 copies per reaction for the N and E gene assays, respectively. RT-ddPCR total process percent recoveries using spiked bovine coronavirus had a mean of 4.12 and a standard deviation (SD) of 5.22.

COVID-19 Case Data. We used dormitory-specific student case status data as the primary outcome variable for our WBE analyses. During the 2020/21 academic year, VT students living in on-campus housing who tested positive for COVID-19 or who were in close-contact to someone who tested positive (as identified via contact tracing) were assigned by the administration to isolation (for diagnosed cases) or quarantine (for those likely exposed to diagnosed cases). These data were received in the form of daily reports (similar to that of hotel bookings) with information on current assignment status (isolation or quarantine), status start and end dates, off- or oncampus housing status, and the names of the dormitories where students were assigned (for isolation) or already residing (for quarantine). See Figure S1 for aggregate assignment data by day of the week and semester.

For our analyses and reporting of results, we used codes in place of names for university dormitories, other buildings, and wastewater sampling sites. The university used one dormitory for housing students assigned to COVID-19 isolation (referred to here as the isolation dormitory or building code 25) as well as a second dormitory when the primary isolation dormitory was at capacity (building code 19). We used building code 99 to represent the sampling point for wastewater outflow from most of the university main campus.

We used a silo-based approach for data management in that only two members of the team interacted with the full and identified data provided by the university administration. Identified data were stored on a secure server, and we used automated code/scripts to remove personal identifiers and extract and collate daily isolation and quarantine counts per building per day for students living in on-campus housing (i.e., the number of new students assigned to isolation or quarantine by building and by day as well as running tallies of the total number of students by assignment status and building).

In addition to these building-specific data, for analysis of wastewater samples from the campus outflow site, we also used data from the university's online COVID-19 dashboard, including the daily number of student positive cases and the daily positive testing rate (these data included results from students residing in on- and off-campus housing).

Building-Specific Occupancy Data. We used data from two sources to estimate daily and weekly occupancy rates by building. Daily estimates were derived from swipe card data from VT buildings with swipe card readers on all external doors. For our primary WBS and WBE analyses (described below), we focused on those dormitories that required the use of a card swipe for entry 24 h/day and for which we had building-specific wastewater sample collection. We also considered analysis of swipe card data from other mixed-use buildings that included student housing as well as other facilities and offices, but because such buildings were open to the public during regular operating/business hours, we were unable to derive sufficiently accurate occupancy estimates. Disaggregated swipe card data for the five VT dormitories we focused on in our study were provided in an automated fashion on a daily basis and included counts for all student and nonstudent unique (i.e., card-specific) and total swipes per day.

In addition to the swipe card data, we also received weekly counts of the number of people assigned to all residential buildings on VT's main campus (provided every Monday for the previous week's data). As part of our analysis, we evaluated associations between these official weekly counts and the swipe card data. Because the swipe data evidenced substantial variance across the week and better accounted for occupancy during weekends and university holidays or breaks, for our primary analyses, we used the swipe card data to estimate daily occupancy on the basis of the total number of swipes per day by students and nonstudents.

Statistical Analyses and Modeling. For the RT-qPCR results, mean Ct values were calculated for each N, E, and S gene measurement by taking the arithmetic mean of the two values for each site by sample, ignoring Ct values of \geq 45 (i.e., nondetects, based on the limit of detection for the assay used)²⁹ and missing values; in instances where only one value was available and the other was a nondetect, the available value was used for the mean ("CTmean_g"). We also created variables for the mean of the Ct means in two ways: when values for all three sites (N, E, and S) were available ("All NES Ct Mean") and a mean of the Ct means derived from all or any available Ct mean data ("Any NES Ct Mean"). In addition, we generated binary variables for each N, E, and S gene mean (detect, nondetect) as well as a binary variable (detect, nondetect) derived from the mean of Ct means ("Any NES Ct Mean as Binary").

We used plate-specific standard curves to calculate estimated viral copies per 100 mL for N, E, and S genes individually (" $ViralCopies_g$ ") as described in eq 1.

Equation for calculating viral copies from RT-qPCR Ct data:

$$ViralCopies_g = 20 \times e \left(\frac{CTmean_g - \beta_p}{\alpha_p} \right)$$
 (1)

where $CTmean_g$ is the arithmetic mean for genes (g), g = N, E, or S; β and α are the beta and y-intercept coefficients from the standard curve from each plate p; 20 is a constant to adjust for the qPCR dilution factor. Nondetect values (Ct \geq 45) were

coded as zeros. After calculating estimated viral copies for N, E, and S genes individually, we created a variable for mean viral copies ("Any NES Mean Viral Copies/100 mL"), calculated in the same fashion as described above for the mean of mean Ct values

For RT-ddPCR runs, samples were considered positive/quantifiable if there were at least three positive droplets per reaction. A reaction was rerun if less than 10 000 total droplets were generated for a PCR reaction. Only those RT-ddPCR N and E viral copy data that were greater than the observation-specific LoD were used for analyses, treating all values below the LoD as zero.

We visually inspected data distributions using histograms as well as QQ-plots to assess normality. We also prespecified that no imputation would take place for missing data (but that we would conduct some missing data/sensitivity analysis for those variables missing >10% of the expected observations).

To adjust Ct and viral copy data by building-specific populations, we used the total unique daily swipe counts per building for students and nonstudents (since nonstudents would also be contributing to the wastewater outflows from the buildings) as well as the weekly occupancy data to calculate mean Ct and estimated viral copies per 100 mL per 100 people by building. To assess potential associations using SARS-CoV-2 signals from the campus outflow sampling site, we used historic data from the university COVID-19 dashboard on the total number of positive tests for students university-wide (as well as the daily positivity rate).

With respect to analyzing associations between Ct and viral copy data and our primary outcome (proxy data for COVID-19 cases by building), we prespecified that, data allowing, we would assess three different approaches to weighting the N, E, and S site data: Equal weighting; 50/25/25 (upweighting N); and learning optimal weights via a machine learning-based approach (which we did not pursue given the relatively low proportion of detects from the RT-qPCR results). While our overarching objective was to analyze the signal from the wastewater with the highest resolution possible, we also planned to analyze the data by discretizing the wastewater results/signal into either trinary (low, medium, high) or binary (detect, nondetect) variables.

For our primary analyses and statistical modeling of the potential association between SARS-CoV-2 signals in the wastewater samples and COVID-19 cases for the five dormitories for which we had high-resolution occupancy and case data, we planned to analyze associations between wastewater samples on day X and corresponding case data on day X + 8 (i.e., using an eight-day lead for the case outcome data). The choice to focus our analyses using an eight-day case lead was informed by an interest in better understanding the potential of WBS as an early warning system, our understanding of COVID-19 research literature on incubation periods at the time we prepared our statistical analysis plan (finalized July, 2021), and our desire to limit the total number of comparisons (models) conducted. Although we prespecified the analysis of case data 8 ± 2 days following wastewater sample collection, given advancements in the understanding of SARS-CoV-2 incubation and shedding dynamics, ^{24,31–33} we modified this to analyze a range of 4 to 9 days after wastewater sampling as well as 3-day bins of cases centered on 8 days. With regard to normalization, we prespecified the use of three normalization schemes (weekly occupancy data, daily swipe card data, and a combination of the two), but on the basis of



Figure 1. Composite sampler surrounded by safety fencing in August of the 2020 fall semester (a), another composite sampler surrounded by safety fencing in January of the 2021 spring semester (b), and a submerged strainer (connected to tubing affixed to a PVC pipe) inside a manhole connected to a composite sampler (c) (photo credits: A. Maile-Moskowitz).

Table 1. Wastewater Samples and SARs-CoV-2 Detection by Gene and Building Codes: RT-qPCR and RT-ddPCR Comparison^a

| | | | bu | building codes for dormitories with site- specific sampling points | | | | building codes for grouped/clustered buildings and sampling points | | | | | campus outflow | | | | | |
|----------|------------------|--------------|----|-----------------------------------------------------------------------|-----|-----|-----|--------------------------------------------------------------------|-----|----|----|----|----------------|----|----|----|-----|-------|
| | gene | SARs-CoV-2 | В8 | B13 | B15 | B17 | B19 | B22 | B25 | G1 | G2 | G3 | G4 | G5 | G6 | G7 | B99 | total |
| RT-qPCR | | not detected | 46 | 41 | 47 | 19 | 16 | 47 | 42 | 46 | 50 | 42 | 41 | 47 | 43 | 46 | 48 | 621 |
| | N | detected | 1 | 6 | 5 | 0 | 0 | 2 | 6 | 3 | 2 | 7 | 6 | 3 | 6 | 2 | 3 | 52 |
| | | total | 47 | 47 | 52 | 19 | 16 | 49 | 48 | 49 | 52 | 49 | 47 | 50 | 49 | 48 | 51 | 673 |
| | | not detected | 44 | 44 | 43 | 19 | 14 | 40 | 39 | 43 | 47 | 40 | 40 | 40 | 45 | 45 | 46 | 589 |
| | \boldsymbol{E} | detected | 3 | 3 | 9 | 0 | 2 | 9 | 9 | 6 | 5 | 9 | 7 | 10 | 4 | 3 | 5 | 84 |
| | | total | 47 | 47 | 52 | 19 | 16 | 49 | 48 | 49 | 52 | 49 | 47 | 50 | 49 | 48 | 51 | 673 |
| | | not detected | 38 | 42 | 37 | 17 | 14 | 37 | 35 | 34 | 37 | 40 | 39 | 37 | 43 | 44 | 34 | 528 |
| | S | detected | 9 | 5 | 15 | 2 | 2 | 12 | 13 | 15 | 15 | 9 | 8 | 13 | 6 | 4 | 17 | 145 |
| | | total | 47 | 47 | 52 | 19 | 16 | 49 | 48 | 49 | 52 | 49 | 47 | 50 | 49 | 48 | 51 | 673 |
| RT-ddPCR | | not detected | 26 | 23 | 19 | 10 | 11 | 15 | 15 | | | | | | | | 9 | 128 |
| | N | detected | 23 | 26 | 32 | 9 | 6 | 33 | 32 | | | | | | | | 40 | 201 |
| | | total | 49 | 49 | 51 | 19 | 17 | 48 | 47 | | | | | | | | 49 | 329 |
| | | not detected | 36 | 36 | 31 | 15 | 15 | 26 | 24 | | | | | | | | 31 | 214 |
| | \boldsymbol{E} | detected | 13 | 13 | 20 | 4 | 2 | 22 | 23 | | | | | | | | 18 | 115 |
| | | total | 49 | 49 | 51 | 19 | 17 | 48 | 47 | | | | | | | | 49 | 329 |

^aNote: RT-qPCR and RT-ddPCR data are from samples collected in the fall 2020 and spring 2021 semesters.

the nature of the occupancy data, we primarily used swipe card data for our analyses.

To assess building-specific associations between SARS-CoV-2 detection in wastewater samples and associated COVID-19 cases, we used random-effects Poisson regression with clusterrobust standard errors (SEs), treating each of the five dormitories in our primary analysis as a cluster (to control for variance within and between clusters). Prior to running the models, data were organized with buildings/clusters serving as

panel variables and the date (daily) as the time variable; unadjusted and population-adjusted viral copy data were log10 transformed, coding nondetects and values < LoD as zero. Beta coefficients from the models were exponentiated to yield incident—rate ratios (IRRs) which, given the underlying structure of the data, may be interpreted as a percentage change in likelihood. SEs and associated *p*-values were calculated using a standard confidence level of 95%.

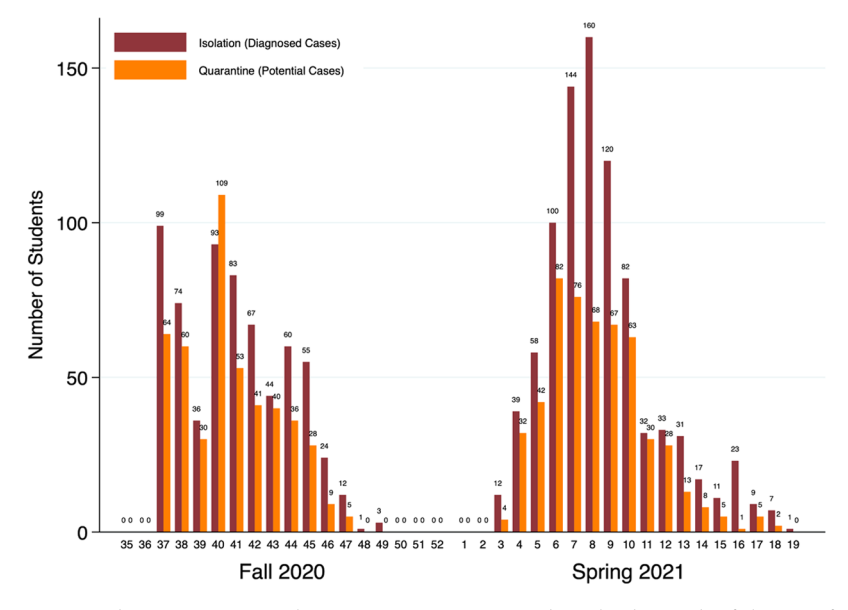


Figure 2. Number of students assigned to COVID-19 isolation or quarantine status by calendar week of the year for five dormitories (building codes B8, B13, B15, B17, and B22).

Table 2. Building Occupancy Estimates by Building/Site Code^a

| | daily swipe card data for students and others | | | | daily swipe card data for students only | | | | weekly occupancy data | | | |
|---------------|-----------------------------------------------|-------|-------|-----|-----------------------------------------|-------|-------|-----|-----------------------|-------|------|-----|
| building code | median | mean | SD | n | median | mean | SD | n | median | mean | SD | n |
| B8 | 424 | 396.3 | 94.0 | 204 | 412 | 386.6 | 91.6 | 204 | 396 | 405.1 | 32.9 | 191 |
| B13 | 418 | 394.1 | 90.3 | 204 | 402 | 380.8 | 88.0 | 204 | 413 | 420.7 | 28.0 | 191 |
| B15 | 443 | 423.2 | 74.5 | 193 | 421 | 404.7 | 70.7 | 193 | 517 | 530.6 | 20.3 | 191 |
| B17 | 63 | 66.3 | 17.6 | 204 | 57 | 61.5 | 17.0 | 204 | 58 | 69.7 | 13.7 | 191 |
| B22 | 727 | 695.7 | 145.4 | 204 | 706 | 675.6 | 143.7 | 204 | 881 | 911.8 | 59.5 | 191 |
| B19 (I-Dorm2) | 32 | 30.5 | 18.9 | 159 | 20 | 20.0 | 16.8 | 159 | 0 | 5.0 | 18.5 | 190 |
| B25 (I-Dorm) | 44 | 45.3 | 20.9 | 193 | 27 | 29.9 | 16.5 | 193 | 16 | 21.7 | 17.1 | 60 |

[&]quot;Notes: Data from the fall 2020 and spring 2021 semesters (excludes data from the 2020/21 winter break). Building code B15 represents data from a cluster of special-purpose on-campus housing with a shared wastewater outflow sampling site/manhole. Due to low occupancy in B17 relative to the other building-sampling sites, wastewater sampling for B17 was discontinued after the fall 2020 semester. I-Dorm = isolation dormitory.

All statistical analyses were conducted using Stata (v16.1; by AC), and primary analyses were replicated using R (4.0.2; by CB).

RESULTS AND DISCUSSION

Wastewater Sample Collection and Assays for SARS-CoV-2 Detection. Over the 2020-2021 academic year, we analyzed 673 wastewater samples collected across the VT campus for SARS-CoV-2 genes N, E, and S using RT-qPCR (Figure 1). As shown in Table 1, across all 673 wastewater samples analyzed for SARS-CoV-2 using RT-qPCR, N, E, and S genes were detected (Ct < 45) in 7.7% (n = 52), 12.5% (n = 84), and 21.6% (n = 145) of samples, respectively.

As discussed previously, following the initial analyses of all RT-qPCR results, 329 samples were independently reanalyzed using RT-ddPCR with the goal of obtaining higher resolution quantification of SARS-CoV-2 genes N and E. Across this subset, N and E genes were detected in 61.1% (n = 201) and 35.0% (n = 115) of samples, respectively. This was a substantial improvement in sensitivity relative to detection by RT-qPCR, where N and E genes had been detected in 7.0% (n = 23) and 12.2%, respectively (n = 40), of this subset of samples. RT-ddPCR LoD data as well as viral copies/100 mL for N and E genes with and without adjustment for LoD (i.e., viral copies if >LoD or if >0) are summarized in Table S2.

Comparisons of the percentages of samples with SARS-CoV-2 detection by building code (and for the outflow site) based on RT-qPCR and RT-ddPCR results are provided in Table S3.

The visual inspection of histograms and QQ-plots for RTddPCR viral copy results for N and E showed right-skewed distributions prior to log-10 transformation (see Figures S2 and S3), as was also the case for RT-qPCR results. RT-ddPCR viral copy results for N and E genes were highly correlated (r =0.967) with slightly higher viral copy concentrations for *E* than for N overall (Figure S4). These RT-ddPCR results and higher average LoD across samples for the E gene (mean = 244, SD = 64) compared with the N gene (mean = 33, SD = 9; see Table S2) were likely due to differences in assay design and target region characteristics. A comparison of viral copy concentrations for RT-ddPCR and RT-qPCR results for N and S (for those samples for which data were available for pairwise comparison) is provided in Figure S5. Unless otherwise noted, all subsequent results and analyses reported herein are based on the RT-ddPCR data (using only observations > LoD).

Building-Specific COVID-19 Case Data and Occupancy Estimation. The cumulative weekly numbers of students from five nonisolation dormitories (building codes 8, 13, 15, 17, and 22) assigned to isolation and quarantine for the fall 2020 and spring 2021 semesters are shown in Figure 2

Table 3. Unadjusted and Population-Adjusted RT-ddPCR Viral Copies/100 mL for N and E Genes by Building

| | | | viral copies | /100 mL | viral copies/100 mL per 100 people: swipe card data (S&O) | | | | viral copies/100 mL per 100 people: housing data (S) | | | | |
|------------------|---------------|--------|--------------|---------|--------------------------------------------------------------|--------|------|--------|------------------------------------------------------|--------|------|--------|----|
| | building code | median | mean | SD | n | median | mean | SD | n | median | mean | SD | n |
| N | B8 | 0 | 331 | 1061 | 49 | 0 | 83 | 276 | 49 | 0 | 88 | 277 | 46 |
| | B13 | 34 | 17 220 | 11 9018 | 49 | 7 | 3901 | 26 927 | 49 | 9 | 4431 | 29 670 | 46 |
| | B15 | 73 | 336 | 628 | 51 | 25 | 80 | 142 | 47 | 20 | 67 | 118 | 47 |
| | B17 | 0 | 110 | 181 | 19 | 0 | 146 | 260 | 19 | 0 | 131 | 219 | 19 |
| | B22 | 101 | 446 | 1208 | 48 | 14 | 58 | 153 | 48 | 12 | 51 | 132 | 45 |
| | B19 (I-Dorm2) | 0 | 255 | 777 | 17 | 0 | 550 | 1708 | 16 | | | | 0 |
| | B25 (I-Dorm) | 165 | 1846 | 6389 | 47 | 357 | 2733 | 7455 | 46 | 571 | 4466 | 10 345 | 16 |
| | outflow | 149 | 232 | 269 | 49 | | | | 0 | | | | 0 |
| \boldsymbol{E} | B8 | 0 | 603 | 2142 | 49 | 0 | 154 | 558 | 49 | 0 | 163 | 559 | 46 |
| | B13 | 0 | 3934 | 24 852 | 49 | 0 | 900 | 5623 | 49 | 0 | 1013 | 6195 | 46 |
| | B15 | 0 | 496 | 856 | 51 | 0 | 118 | 191 | 47 | 0 | 99 | 161 | 47 |
| | B17 | 0 | 68 | 145 | 19 | 0 | 86 | 176 | 19 | 0 | 81 | 171 | 19 |
| | B22 | 0 | 1076 | 3705 | 48 | 0 | 139 | 466 | 48 | 0 | 122 | 401 | 45 |
| | B19 (I-Dorm2) | 0 | 746 | 2905 | 17 | 0 | 1724 | 6369 | 16 | | | | 0 |
| | B25 (I-Dorm) | 0 | 2312 | 5698 | 47 | 173 | 3828 | 8937 | 46 | 0 | 5566 | 14 154 | 16 |
| | outflow | 0 | 260 | 406 | 49 | | | | 0 | | | | 0 |

"Notes: Data from the fall 2020 and spring 2021 semesters. I-Dorm = COVID-19 isolation dormitory. S = students. S&O = students and others.

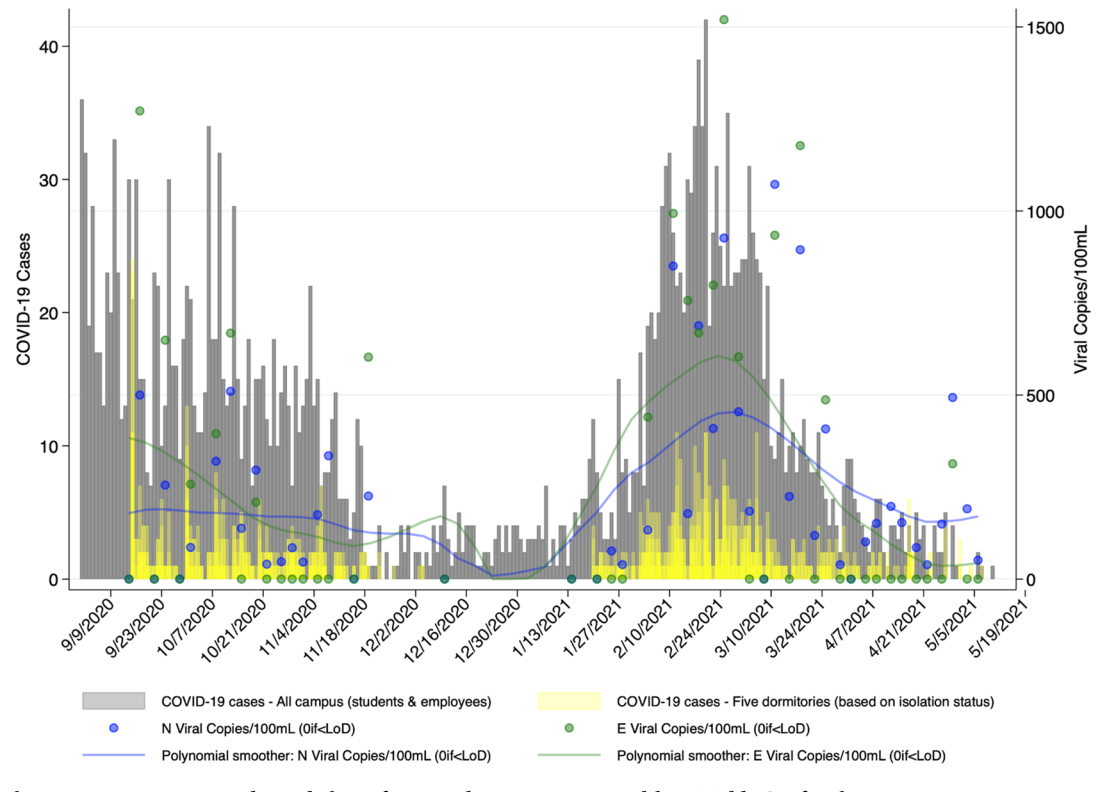


Figure 3. Viral copy concentrations and trends lines for N and E genes measured by RT-ddPCR for the university wastewater outflow site and COVID-19 cases university-wide (gray) and for students in the five dormitories analyzed in this study (yellow). Note: N and E trend lines were fit using polynomial smoothing.

(assignment to isolation and quarantine by day of the week and semester shown in Figure S1).

During the fall 2020 semester at VT, in response to the COVID-19 pandemic, courses were scheduled to resume in an online format following the November Thanksgiving holiday. Consequently, most students residing on campus left before the holiday break began on November 21, 2020; this shift in on-campus residency is reflected in the isolation and quarantine data in Figure 2 for the 47th and 48th weeks of the calendar year. Aggregated occupancy estimates by building

code derived from daily swipe card data for students and others, students only, and based on weekly counts are summarized for the fall and spring semesters in Table 2 based on occupancy data from September 1, 2020 through November 25, 2020 and from January 15, 2021 through May 13, 2021. The large SDs observed (relative to the means) for the swipe card data are due primarily to inter- and intraweekly variation as well as relative decreases in student occupancy in the weeks before and after the winter break between semesters, as shown in Figure S6 for the five nonisolation dormitories.

Population-Adjusted SARS-CoV-2 Data. As shown in Table 3, among the subset of sampling sites analyzed using RT-ddPCR, mean SARS-CoV-2 viral copies were the highest for both N and E genes in samples collected from dormitory code B13 (17 220 and 3934 copies/100 mL for N and E, respectively) as well as the primary isolation dormitory (1846 and 2312 copies/100 mL for N and E, respectively, at site B25). After the adjustment of copy numbers based on the estimated populations contributing to wastewater outflows from these buildings, mean viral copies/100 mL/100 people were still the highest for dormitory B13 for N (3901 copies/ 100 mL/100 people) but not for E (900 copies/100 mL/100 people), followed by the population-adjusted means for the isolation dormitory, which were higher than the unadjusted copy numbers (2733 and 3828 copies/100 mL/100 people for N and E, respectively). Similar trends were observed for population-adjusted means using the weekly housing count data.

One would expect mean SARS-CoV-2 viral copy numbers to be higher on a per capita basis for samples collected from COVID-19 isolation dormitories given the higher rates of infection and viral shedding. Indeed, when comparing unadjusted and population adjusted (based on swipe card data) viral copy means across all sites (Table 3), aside from a slight increase in the population-adjusted mean for B17 (33%, from 110 to 146, for N; 26%, from 68 to 86, for E; though samples were only collected for B17 during the fall semester), population-adjusted means were lower than the unadjusted means for all nonisolation dormitories. Conversely, for the primary isolation dormitory, population-adjusted viral copy means were 48% and 66% higher than the unadjusted viral copy means for N and E (from 1846 to 2733 and from 2312 to 3828, respectively) and 116% and 131% higher for the secondary isolation dormitory for the same comparison of viral copy means for N and E (from 255 to 550 and from 746 to 1724, respectively). These trends were also observed for viral copy means when adjusted (data allowing) using the weekly housing data.

As shown in Figure S7, the overall distribution of SARS-CoV-2 viral copy numbers for N and E for the five dormitories generally aligns with corresponding COVID-19 case data (based on isolation assignment by building) for the time period assessed, with a more pronounced overlap observed for the spring 2021 semester. Case data overlaid with population-adjusted (based on swipe card data) viral copy numbers are shown in Figure S8. For the RT-qPCR results, less-pronounced but somewhat similar trends were observed for the population-adjusted viral copy concentrations for N, E, and S genes, as shown in Figure S9.

Looking at results from the campus wastewater outflow samples, as shown in Figure 3, trend lines for SARS-CoV-2 viral copy numbers for N and E follow a pattern similar to that of COVID-19 case counts based on isolation data for the five dormitories analyzed in this study as well as for diagnosed cases university-wide, particularly so for the spring 2021 semester. Population-adjusted viral copies from wastewater samples collected from the university's main COVID-19 isolation dormitory also aligned with these COVID-19 case trends (Figure S10).

Statistical Modeling and Wastewater-Based Epidemiology. For our initial models, we used an eight-day lead for building-specific COVID-19 cases (the outcome variable, derived from isolation assignment status). As shown in Table

4, using random-effects Poisson regression with cluster-robust SEs, we observed positive (i.e., increases in the likelihood) and

Table 4. Random-Effects Poisson Regression with Cluster-Robust Standard Errors Using COVID-19 Cases 8 days after Wastewater Sampling as the Outcome Variable^a

| model: predictor variable | IRR | SE | <i>p</i> -value | n | clusters (buildings) |
|---------------------------------------------------------------|-------|-------|-----------------|-----|-------------------------|
| N: log10 viral copies/ 100 mL (ND = 0) | 1.199 | 0.096 | 0.024 | 215 | 5 |
| E: log10 viral copies/ 100 mL (ND = 0) | 1.220 | 0.101 | 0.017 | 215 | 5 |
| N: log10 viral copies/ 100 mL/100 ppl, swipe (ND = 0) | 1.206 | 0.061 | <0.001 | 211 | 5 |
| E: log10 viral copies/ 100 mL/100 ppl, swipe (ND = 0) | 1.265 | 0.082 | <0.001 | 211 | 5 |
| N: log10 viral copies/ 100 mL/100 ppl, housing (ND = 0) | 1.168 | 0.060 | 0.002 | 202 | 5 |
| E: log10 viral copies/ 100 mL/100 ppl, housing (ND = 0) | 1.233 | 0.087 | 0.003 | 202 | 5 |
| N: viral copies as binary (ND vs detected) | 1.845 | 0.454 | 0.013 | 215 | 5 |
| E: viral copies as binary (ND vs detected) | 1.994 | 0.508 | 0.007 | 215 | 5 |

"Notes: Analysis using RT-ddPCR data from samples collected in the fall 2020 and spring 2021 semesters. COVID-19 case data are based on building-specific student assignment to COVID-19 isolation status. log10 = log-10 transformed (ND and <LoD = 0). ND = not detected. Ppl = people.

statistically significant (at a p = 0.05 threshold) associations with COVID-19 cases 8 days following sample collection for log10 transformed viral copies/100 mL for N and E genes. IRRs from analysis of log10 transformed population-adjusted viral copy concentrations (based on swipe card and weekly housing data) for N and E were also positive and statistically significant. In particular, one-log increases in swipe-normalized viral copies for N and E were associated with statistically significant increases of 21% and 27% in the likelihood of observing COVID-19 cases 8 days after sample collection (IRR = 1.206, p < 0.001, n = 211 for N; IRR = 1.265, p < 0.001, n = 1.206211 for E). We also analyzed these associations using binary variables for N and E (not detected = 0, detected = 1), and we observed associations with COVID-19 cases that were also clinically and statistically significant. Specifically, the detection of N genes in wastewater samples was associated with an 85% increase in the likelihood of COVID-19 cases 8 days later (IRR = 1.845, p = 0.013, n = 215), and the detection of E genes in wastewater samples was associated with a 99% increase in the likelihood of COVID-19 cases 8 days later (IRR = 1.994, p = 0.007, n = 215).

Because the method of sample collection (composite vs grab) could be expected to impact our overall findings, we also ran each of the models presented in Table 4 with a binary covariate to control for the potential impacts of the sampling method (composite = 0, grab = 1). As shown in Table S4, after controlling for the type of sampling method, the direction and significance (at a p=0.05 threshold) of IRRs remained unchanged across all eight models, and the size of IRRs, SEs, and associated p-values remained very similar with unadjusted (Table 4) and adjusted (Table S4) IRRs differing by a range of only 0.16% to 3.04% (mean = 1.20%, SD = 1.02%).

Results for models based on RT-qPCR data from the same subset of wastewater samples are provided in Table S5. Across these models, all IRRs were less than one, indicating negative associations between log10 transformed viral copies for N, E, and S in isolation or when combined (population-adjusted and unadjusted) and COVID-19 cases 8 days following sample collection. Across models with the RT-qPCR data, only the IRR for log10 transformed viral copies for N was statistically significant (IRR = 0.146, p < 0.001, n = 212; incidentally, this was also the lowest IRR observed across models in Table S5). When the association was analyzed using a binary predictor ("Any NES Ct Mean as Binary"), the IRR was close to the null and not significant (IRR = 0.996, p = 0.992, n = 213).

To evaluate associations between SARS-CoV-2 in wastewater samples and COVID-19 cases 7, 8, and 9 days following wastewater sampling, we used the same random-effects Poisson regression models and variables in Table 4, but for the outcome variable, we used 3-day bins of cases centered on 8 days following wastewater sampling (8 \pm 1 day). As shown in Table S6, resulting IRRs were positive for all models using log-10 transformed viral copies as predictors but only statistically significant for population-adjusted (based on swipe card data) viral copies for the E gene (IRR = 1.158, p = 0.038, n = 212). When using a binary predictor for N and E (not detected = 0, detected = 1), IRRs for the 3-day bin of cases were both positive, suggesting a 24% and 55% increase in the likelihood of COVID-19 cases for N and E detection, respectively, but the association was only statistically significant for E (IRR = 1.241 p = 0.270, n = 216 for N; IRR = 1.549, p = 0.012, n = 216 for E).

The analyses of binary variables for N and E and COVID-19 cases 4 to 9 days (8 days also already presented in Table 4) following wastewater sample collection are provided in Table 5. IRRs were statistically significant using five-, six-, and eightday leads, with the largest observed IRRs at 5 days (IRR = 2.136, p < 0.001, n = 216 and IRR = 2.313, p < 0.001, n = 216for N and E, respectively) and 8 days (IRR = 1.845, p = 0.013, n = 215 and IRR = 1.994, p = 0.007, n = 215 for N and E, respectively) after wastewater sampling. Running the same swipe card based model shown in Table 4 but using a five-day rather than eight-day lead, we observed that one-log increases in swipe-normalized viral copies for N and E were associated with statistically significant increases of 40% and 43% in the likelihood of observing COVID-19 cases 5 days after sample collection (IRR = 1.403, SE = 0.157, p = 0.002, n = 212 for N; IRR = 1.426, SE = 0.112, p < 0.001, n = 212 for E).

Compared with the size and direction of the IRRs at sevenand nine-day leads, the eight-day lead yielded larger and more significant effect sizes. As a sensitivity analysis, we ran the seven-, eight-, and nine-day models using data on student assignment to isolation and assignment to quarantine status as our COVID-19 case outcome variable. As shown in Table S7 with this broader proxy of COVID-cases as the outcome variable, the IRRs increased slightly when using seven- and eight-day leads but decreased slightly for N when using a nineday lead (compared with results in Table 5), and the associations were again only statistically significant at an eight-day lead. Finally, we analyzed data from the RT-qPCR results using binary variables for the detection of N, E, and/or S Ct values and COVID-19 cases as the outcome (using only isolation status) 8 ± 2 days following wastewater sampling (Table S8). At an eight-day lead, the IRR was essentially null and not statistically significant (IRR = 0.996, p = 0.992, n = 0.992

Table 5. Random-Effects Poisson Regression with Cluster-Robust Standard Errors Where the Outcome Variable is the Number of COVID-19 Cases 4 to 9 Days after Wastewater Sampling Using RT-ddPCR Results as the Predictor^a

| model: predictor variable | IRR | SE | p-value | n | clusters (buildings) |
|----------------------------------------------------|-------|-------|---------|-----|-------------------------|
| N: viral copies as binary (ND vs detected), 4 days | 0.905 | 0.437 | 0.836 | 216 | 5 |
| E: viral copies as binary (ND vs detected), 4 days | 1.594 | 0.904 | 0.411 | 216 | 5 |
| N: viral copies as binary (ND vs detected), 5 days | 2.136 | 0.246 | <0.001 | 216 | 5 |
| E: viral copies as binary (ND vs detected), 5 days | 2.313 | 0.517 | <0.001 | 216 | 5 |
| N: viral copies as binary (ND vs detected), 6 days | 1.739 | 0.344 | 0.005 | 216 | 5 |
| E: viral copies as binary (ND vs detected), 6 days | 1.901 | 0.551 | 0.027 | 216 | 5 |
| N: viral copies as binary (ND vs detected), 7 days | 0.818 | 0.562 | 0.770 | 216 | 5 |
| E: viral copies as binary (ND vs detected), 7 days | 1.083 | 0.781 | 0.912 | 216 | 5 |
| N: viral copies as binary (ND vs detected), 8 days | 1.845 | 0.454 | 0.013 | 215 | 5 |
| E: viral copies as binary (ND vs detected), 8 days | 1.994 | 0.508 | 0.007 | 215 | 5 |
| N: viral copies as binary (ND vs detected), 9 days | 1.112 | 0.219 | 0.587 | 215 | 5 |
| E: viral copies as binary (ND vs detected), 9 days | 1.527 | 0.423 | 0.127 | 215 | 5 |
| | | | | | |

^aNotes: Analysis using RT-ddPCR data from samples collected in the fall 2020 and spring 2021 semesters. COVID-19 case data are based on building-specific student assignment to COVID-19 isolation status. ND = not detected.

213), but was positive and statistically significant for the nine-day lead (IRR = 1.868, p = 0.023, n = 213).

On the basis of these results (Tables 4 and 5), in Figure 4, population-adjusted viral copy concentrations for *N* and *E* (copies/100 mL/100 people based on swipe card data) are plotted over COVID-19 cases using an eight-day lead (i.e., building-linked SARS-CoV-2 RT-ddPCR results and associated assignment of students to isolation status) with polynomial smoothers to show trend lines for *N* and *E* over the study period. These results are shown disaggregated by dormitory in Figure 5. Figure S11 provides a comparison of population-adjusted viral copy concentration trends between RT-ddPCR and RT-qPCR measurements (using polynomial smoothers) overlaid with COVID-19 case data with an eight-day lead.

Study Limitations. The layout of many sewers precluded the use of composite samples (e.g., as for B19 and B25) or flow meters. Low flows at times in many sewers (late night and early morning hours in particular) contributed to battery depletion for some composite samplers (an issue compounded by low temperatures during the winter months); in such instances, grab samples were used to supplement the volume collected. Due to relatively low occupancy and low wastewater flow in B17, sampling was discontinued after the fall 2020 semester. At times, heterogeneity of the wastewater composition and flow temporarily interfered with sampling equipment (e.g., when toilet paper caught onto sampling tubes/strainers). Logistical constraints (e.g., malfunctioning samplers, construction preventing access to manholes) also prevented the consistent collection of samples from all sites on all sampling days.

Working with a clinical lab that was simultaneously processing large numbers of COVID-19 testing swabs for the

ı

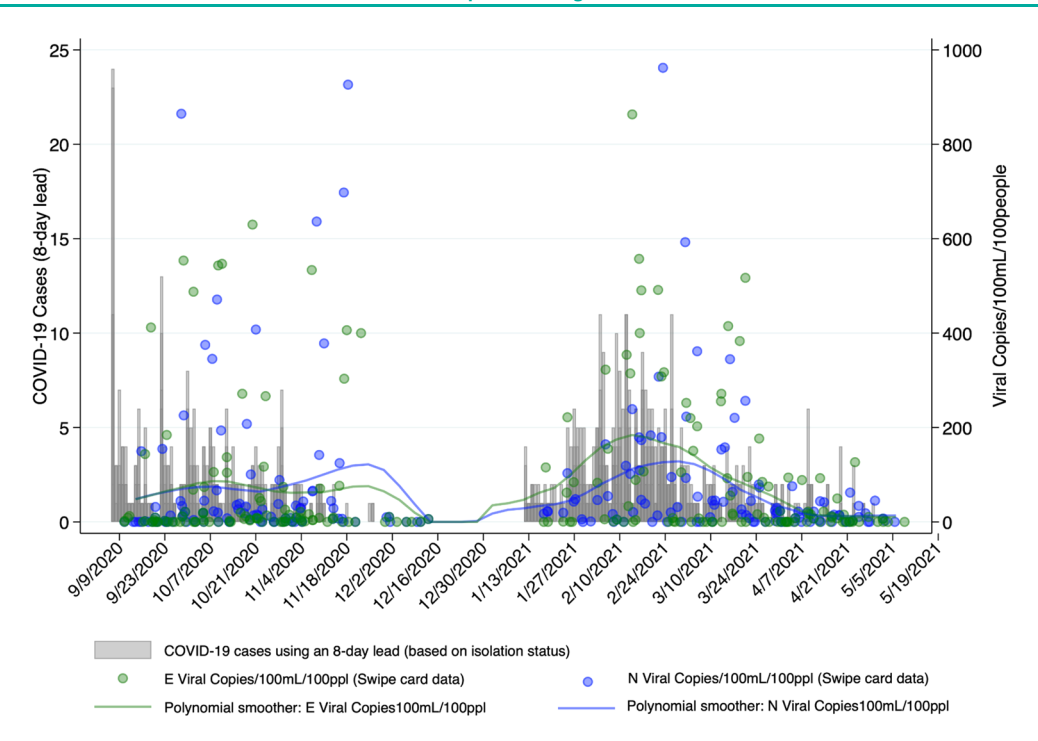


Figure 4. Population-adjusted viral copy concentrations and trend lines for N and E genes measured by RT-ddPCR and COVID-19 cases with an eight-day lead for five dormitories. Notes: Three N observations and five E observations were removed for improved visualization. Jitter = 3. Ppl = people. N and E trend lines were fit using polynomial smoothing. Population adjustment was based on swipe card data.

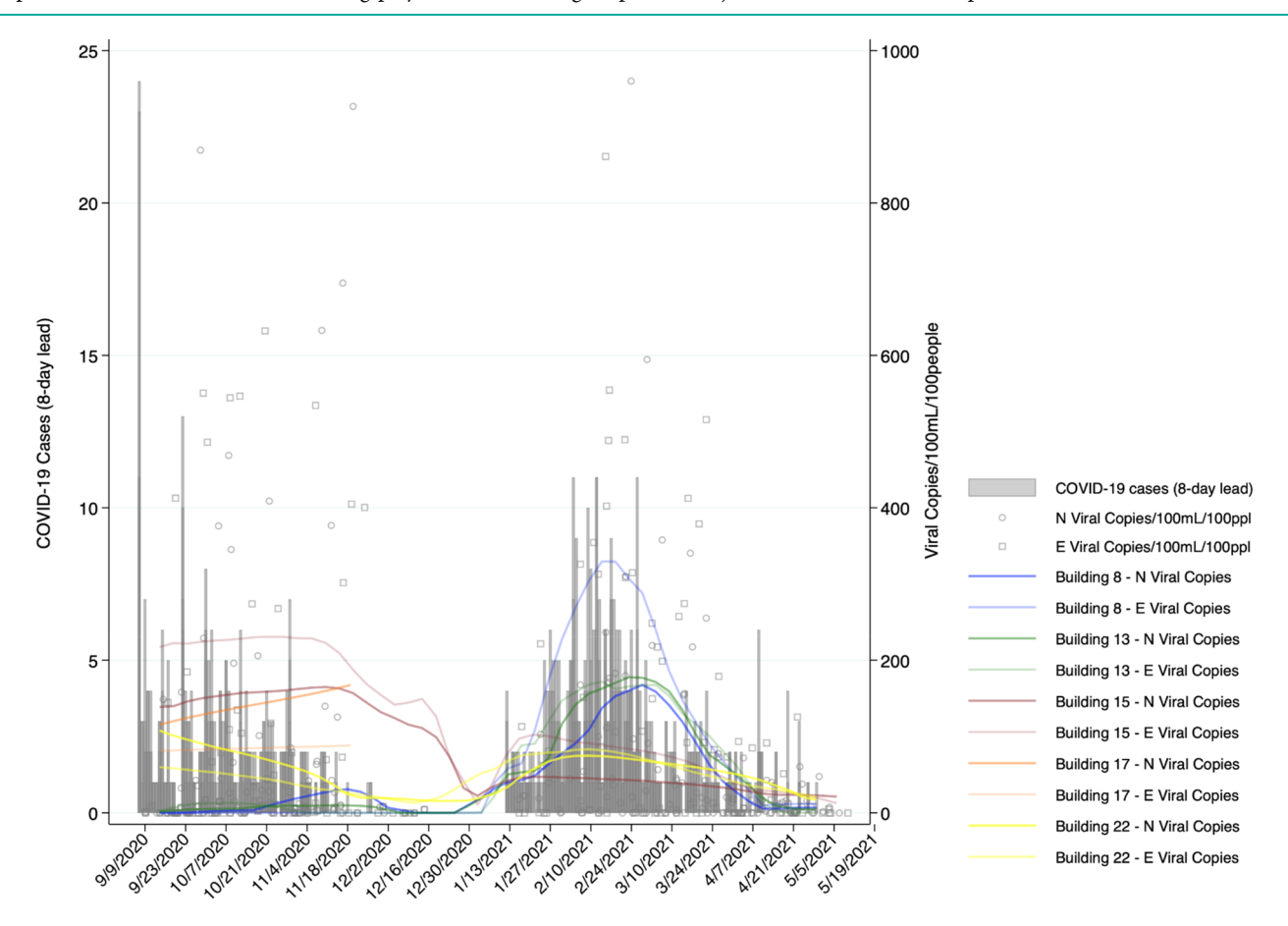


Figure 5. Population-adjusted viral copy concentrations and dormitory specific trend lines for N and E genes measured by RT-ddPCR and COVID-19 cases with an eight-day lead for five dormitories. Notes: Three N observations and five E observations were removed for improved visualization. Jitter = 3. Ppl = people. Population adjustment was based on swipe card data. N and E trend lines were fit using polynomial smoothing.

university allowed for a rapid start to the project as well as the benefit of using the same assay for both clinical and wastewater samples. However, the clinical lab's RT-qPCR techniques were not optimized for wastewater samples, and due to their heavy workload, there were few opportunities to reanalyze samples or optimize methods for the analysis of environmental samples. It was not feasible, for example, to analyze multiple dilutions or conduct additional tests to evaluate the potential impacts of concentrated inhibitors on RT-qPCR amplification or false negative results (though we were able to address these issues through a focused reanalysis of a subset of samples using RT-ddPCR).

With regard to the COVID-19 isolation status data, for some students (<15%), their temporary room assignments changed one or more times throughout the duration of their assignment to isolation, which added uncertainty to some of our estimates of daily occupancy for the isolation dormitories, and by extension to estimates of population-adjusted viral copy numbers for the isolation dormitories. However, there were few such issues with data for the start date of isolation status assignments (the primary data point used for our estimation of COVID-19 cases by date and building). Finally, given the nature of the RT-qPCR results and relatively limited number of observations with Ct values <45 for *N*, *E*, and *S*, we did not have sufficient data to adequately compare equal weightings for *N*, *E*, and *S* with a weighting scheme that upweighted results for *N*.

■ RESULTS IN CONTEXT AND IMPLICATIONS

According to information collated by researchers at UC Merced, 21 as of January 2022, more than 250 universities worldwide were using, or had used, SARS-CoV-2 WBS. To help contextualize our use of data and methods for this initiative at VT, we conducted a nonsystematic review of published peer-reviewed articles describing results from COVID-19 WBS initiatives at universities and colleges in the USA and Canada and extracted summary information on methods from six such publications^{34–39} (see Table S9). Across these universities, the number of wastewater sampling sites ranged from 1 to 68; sample collection frequencies ranged from 1 to 7 days/week, and three of the six universities used composite samplers, while the others used grab samples. All six used RT-qPCR for SARS-CoV-2 detection with some analyzing only N genes and others analyzing N and E. The methods used for concentrating samples as well as the type of recovery controls varied across the studies, as did methods for assessing inhibition (when reported). Normalization was based primarily on the use of human fecal markers or flow/volume (for additional details, see Table S9). More broadly, we did not identify any published university-focused studies that used building-specific occupancy and COVID-19 case data at a daily resolution for WBS or WBE, as was the focus of our study, and only a few that used statistical modeling for WBE.

Our study identified marked associations between the SARS-CoV-2 signals measured from campus outflow wastewater samples and university-wide COVID-19 case data as well as similar trends for the five nonisolation dormitories. The clinically and statistically significant associations we observed between population-adjusted SARS-CoV-2 signals in wastewater samples and corresponding COVID-19 case data 8 days following sample collection, as well as the higher population-adjusted viral concentrations observed in samples from the university's COVID-19 isolation dormitories, provide addi-

tional evidence and a concrete framework for the application of WBS to quantitatively predict COVID-19 trends at subsewershed scales, such as a university campus.

Compared with published methods and results from other university-scale COVID-19 WBS initiatives (as of January 2022), our study appeared to be relatively unique with respect to our use of building-specific occupancy and COVID-19 case data to calculate population-adjusted SARS-CoV-2 results as well as our use of statistical modeling to assess associations between SARS-CoV-2 signals from wastewater samples and subsequent COVID-19 infections. We expect that through improved modeling of the relationships between SARS-CoV-2 genes measured in sewage and associated COVID-19 infection data at subsewershed scales, this framework and approach can help to advance WBS and WBE efforts at building-specific, subsewershed, and sewershed scales.

ASSOCIATED CONTENT

Solution Supporting Information

The Supporting Information is available free of charge at https://pubs.acs.org/doi/10.1021/acsestwater.2c00059.

Additional figures: isolation and quarantine assignment data by day of week and semester; histograms and QQplots of RT-ddPCR data before and after log-10 transformation; scatterplots of RT-ddPCR and RTqPCR data for N and E genes; aggregated occupancy data by week of the year and source; RT-ddPCR and RT-qPCR viral copy concentrations and cases with and without population adjustment for five buildings and university-wide; additional tables: wastewater sampling methods by day of week and semester; LoD data for RTddPCR results; RT-ddPCR and RT-qPCR results and comparison by building/site; statistical modeling results with RT-qPCR data controlling for the sampling method, with RT-qPCR data using 3-day bins of cases $(8 \pm 1 \text{ day})$ and isolation and quarantine outcomes, and for RT-qPCR data at 6-10 days leads; comparison of university-focused wastewater surveillance methods from selected publications (PDF)

AUTHOR INFORMATION

Corresponding Author

Peter J. Vikesland — Department of Civil and Environmental Engineering, Virginia Tech, Blacksburg, Virginia 24061, United States; Orcid.org/0000-0003-2654-5132; Email: pvikes@vt.edu

Authors

Alasdair Cohen — Department of Population Health Sciences, Virginia Tech, Blacksburg, Virginia 24061, United States; Department of Civil and Environmental Engineering, Virginia Tech, Blacksburg, Virginia 24061, United States; orcid.org/0000-0002-9917-8647

Ayella Maile-Moskowitz – Department of Civil and Environmental Engineering, Virginia Tech, Blacksburg, Virginia 24061, United States

Christopher Grubb – Department of Statistics, Virginia Tech, Blacksburg, Virginia 24061, United States

Raul A. Gonzalez – Hampton Roads Sanitation District, Virginia Beach, Virginia 23455, United States; o orcid.org/ 0000-0002-8115-7709

- Alessandro Ceci Molecular Diagnostics Laboratory, Fralin Biomedical Research Institute, Virginia Tech, Roanoke, Virginia 24016, United States
- Amanda Darling Department of Population Health Sciences, Virginia Tech, Blacksburg, Virginia 24061, United States; Department of Civil and Environmental Engineering, Virginia Tech, Blacksburg, Virginia 24061, United States
- Laura Hungerford Department of Population Health Sciences, Virginia Tech, Blacksburg, Virginia 24061, United States
- Ronald D. Fricker, Jr. Department of Statistics, Virginia Tech, Blacksburg, Virginia 24061, United States
- Carla V. Finkielstein Molecular Diagnostics Laboratory, Fralin Biomedical Research Institute, Virginia Tech, Roanoke, Virginia 24016, United States; Integrated Cellular Responses Laboratory, Fralin Biomedical Research Institute at VTC, Roanoke, Virginia 24016, United States; Department of Biological Sciences, Virginia Tech, Blacksburg, Virginia 24061, United States
- Amy Pruden Department of Civil and Environmental Engineering, Virginia Tech, Blacksburg, Virginia 24061, United States; orcid.org/0000-0002-3191-6244

Complete contact information is available at: https://pubs.acs.org/10.1021/acsestwater.2c00059

Funding

This study was primarily supported through internal funding from Virginia Tech. Additional funds were provided through the National Science Foundation (NSF) OISE award (#1545756), ECCSS NNCI award (#1542100), CSSI award (#2004751), and NRT award (#2125798). Funding was also provided by the Center for Science and Engineering of the Exposome at the Virginia Tech Institute for Critical Technology and Applied Science (ICTAS).

Notes

The authors declare no competing financial interest. The data underlying this study are not publicly available due to the potential to link COVID-19 case data to specific dates and dormitories and to combine such information with online data sources to potentially reidentify personally identifiable information.

ACKNOWLEDGMENTS

This work and research was made possible thanks to the support and contributions of many people across Virginia Tech. In particular, the authors extend their thanks to Michael Mulhare, Jennifer Averill, and Andrew Marinik (Emergency Management); Bobby Polly (Planning, Infrastructure & Facilities); Jean Luyendijk and Julie Wesel (Hokie Passport Services); Nickie Smith (Housing Services); David Higdon and Leanna House (Statistics); Rachel Silverman and Danielle Short (Population Health Sciences); Kimberly Ascue, Richard Clutter, and Jeremy Larose (Information Systems & IT); Navid Ghaffarzadegan, and other members of the VT COVID-19 Modeling Group.

REFERENCES

- (1) Metcalf, T. G.; Melnick, J. L.; Estes, M. K. Environmental Virology From Detection of Virus in Sewage and Water by Isolation to Identification by Molecular Biology—A Trip of Over 50 Years. *Annu. Rev. Microbiol.* **1995**, 49 (1), 461–487.
- (2) Daughton, C. G. Illicit Drugs in Municipal Sewage Proposed New Nonintrusive Tool to Heighten Public Awareness of Societal

- Use of Illicit-Abused Drugs and Their Potential for Ecological Consequences. *Pharm. Care Prod. Environ.* **2001**, 791, 348–364.
- (3) Zuccato, E.; Chiabrando, C.; Castiglioni, S.; Calamari, D.; Bagnati, R.; Schiarea, S.; Fanelli, R. Cocaine in Surface Waters: A New Evidence-Based Tool to Monitor Community Drug Abuse. *Environ. Health Glob. Access Sci. Source* **2005**, *4*, 14–14.
- (4) Lago, P. M.; Gary, H. E.; Pérez, L. S.; Cáceres, V.; Olivera, J. B.; Puentes, R. P.; Corredor, M. B.; Jímenez, P.; Pallansch, M. A.; Cruz, R. G. Poliovirus Detection in Wastewater and Stools Following an Immunization Campaign in Havana, Cuba. *Int. J. Epidemiol.* **2003**, 32 (5), 772–777.
- (5) Lodder, W.; de Roda Husman, A. M. SARS-CoV-2 in Wastewater: Potential Health Risk, but Also Data Source. *Lancet Gastroenterol. Hepatol.* **2020**, *5* (6), 533–534.
- (6) Zhang, Y.; Cen, M.; Hu, M.; Du, L.; Hu, W.; Kim, J. J.; Dai, N. Prevalence and Persistent Shedding of Fecal SARS-CoV-2 RNA in Patients With COVID-19 Infection: A Systematic Review and Meta-Analysis. Clin. Transl. Gastroenterol. 2021, 12 (4), No. e00343.
- (7) Park, M.; Won, J.; Choi, B. Y.; Lee, C. J. Optimization of Primer Sets and Detection Protocols for SARS-CoV-2 of Coronavirus Disease 2019 (COVID-19) Using PCR and Real-Time PCR. *Exp. Mol. Med.* 2020 526 **2020**, 52 (6), 963–977.
- (8) WHO. Diagnostic Testing for SARS-CoV-2: Interim Guidance; WHO: Geneva, September 11, 2020.
- (9) CDC. CDC 2019-Novel Coronavirus (2019-NCoV) Real-Time RT-PCR Diagnostic Panel, For Emergency Use Only, Instructions for Use; CDC: Atlanta, 2020.
- (10) Won, J.; Lee, S.; Park, M.; Kim, T. Y.; Park, M. G.; Choi, B. Y.; Kim, D.; Chang, H.; Kim, V. N.; Lee, C. J. Development of a Laboratory-Safe and Low-Cost Detection Protocol for SARS-CoV-2 of the Coronavirus Disease 2019 (COVID-19). *Exp. Neurobiol.* **2020**, 29 (2), 107–107.
- (11) Alsuhaibani, M. A.; Kobayashi, T.; Trannel, A.; Holley, S.; Abosi, O. J.; Jenn, K. E.; Meacham, H.; Sheeler, L.; Etienne, W.; Dains, A.; Kukla, M. E.; Ward, E.; Ford, B.; Edmond, M. B.; Wellington, M.; Diekema, D. J.; Salinas, J. L. Coronavirus Disease 2019 (COVID-19) Admission Screening and Assessment of Infectiousness at an Academic Medical Center in Iowa, 2020. Infect. Control Hosp. Epidemiol. 2021, 1–5.
- (12) Medema, G.; Heijnen, L.; Elsinga, G.; Italiaander, R.; Brouwer, A. Presence of SARS-Coronavirus-2 RNA in Sewage and Correlation with Reported COVID-19 Prevalence in the Early Stage of the Epidemic in The Netherlands. *Environ. Sci. Technol. Lett.* **2020**, 7, 511. (13) Jahn, K.; Dreifuss, D.; Topolsky, I.; Kull, A.; Ganesanandamoorthy, P.; Fernandez-Cassi, X.; Bänziger, C.; Stachler, E.; Fuhrmann, L.; Philipp Jablonski, K.; Chen, C.; Aquino, C.; Stadler, T.; Ort, C.; Kohn, T.; Julian, T. R.; Beerenwinkel, N. Detection of SARS-CoV-2 Variants in Switzerland by Genomic Analysis of Wastewater Samples. *medRxiv* **2021**, 2021.01.08.21249379; DOI: 10.1101/2021.01.08.21249379.
- (14) La Rosa, G.; Iaconelli, M.; Mancini, P.; Bonanno Ferraro, G.; Veneri, C.; Bonadonna, L.; Lucentini, L.; Suffredini, E. First Detection of Sars-Cov-2 in Untreated Wastewaters in Italy. *Sci. Total Environ.* **2020**, 736 (20), 139652.
- (15) Sharif, S.; Ikram, A.; Khurshid, A.; Salman, M.; Mehmood, N.; Arshad, Y.; Ahmed, J.; Safdar, R. M.; Rehman, L.; Mujtaba, G.; Hussain, J.; Ali, J.; Angez, M.; Alam, M. M.; Akthar, R.; Malik, M. W.; Baig, M. Z. I.; Rana, M. S.; Usman, M.; Ali, M. Q.; Ahad, A.; Badar, N.; Umair, M.; Tamim, S.; Ashraf, A.; Tahir, F.; Ali, N. Detection of SARs-CoV-2 in Wastewater Using the Existing Environmental Surveillance Network: A Potential Supplementary System for Monitoring COVID-19 Transmission. *PLoS One* **2021**, *16* (6), No. e0249568.
- (16) Ahmed, W.; Tscharke, B.; Bertsch, P. M.; Bibby, K.; Bivins, A.; Choi, P.; Clarke, L.; Dwyer, J.; Edson, J.; Nguyen, T. M. H.; O'Brien, J. W.; Simpson, S. L.; Sherman, P.; Thomas, K. V.; Verhagen, R.; Zaugg, J.; Mueller, J. F. SARS-CoV-2 RNA Monitoring in Wastewater as a Potential Early Warning System for COVID-19 Transmission in

- the Community: A Temporal Case Study. Sci. Total Environ. 2021, 761, 144216-144216.
- (17) Virginia Tech. Virginia Tech Fall 2020 COVID-19 Operational Plan; Virginia Tech: Blacksburg, 2020.
- (18) Virginia Tech. Virginia Tech Spring 2021 COVID-19 Operational Plan; Virginia Tech: Blacksburg, 2021.
- (19) Betancourt, W. Q.; Schmitz, B. W.; Innes, G. K.; Prasek, S. M.; Pogreba Brown, K. M.; Stark, E. R.; Foster, A. R.; Sprissler, R. S.; Harris, D. T.; Sherchan, S. P.; Gerba, C. P.; Pepper, I. L. COVID-19 Containment on a College Campus via Wastewater-Based Epidemiology, Targeted Clinical Testing and an Intervention. *Sci. Total Environ.* **2021**, 779, 146408.
- (20) Harris-Lovett, S.; Nelson, K. L.; Beamer, P.; Bischel, H. N.; Bivins, A.; Bruder, A.; Butler, C.; Camenisch, T. D.; Long, S. K. D.; Karthikeyan, S.; Larsen, D. A.; Meierdiercks, K.; Mouser, P. J.; Pagsuyoin, S.; Prasek, S. M.; Radniecki, T. S.; Ram, J. L.; Roper, D. K.; Safford, H.; Sherchan, S. P.; Shuster, W.; Stalder, T.; Wheeler, R. T.; Korfmacher, K. S. Wastewater Surveillance for SARS-CoV-2 on College Campuses: Initial Efforts, Lessons Learned, and Research Needs. Int. J. Environ. Res. Public Health 2021, 18 (9), 4455–4455.
- (21) UC Merced. COVIDPoops19 Dashboard; https://www.arcgis.com/apps/dashboards/c778145ea5bb4daeb58d31afee389082 (accessed 2022-01-25).
- (22) Sims, N.; Kasprzyk-Hordern, B. Future Perspectives of Wastewater-Based Epidemiology: Monitoring Infectious Disease Spread and Resistance to the Community Level. *Environ. Int.* **2020**, 139, 105689.
- (23) Kumblathan, T.; Liu, Y.; Uppal, G. K.; Hrudey, S. E.; Li, X.-F. Wastewater-Based Epidemiology for Community Monitoring of SARS-CoV-2: Progress and Challenges. *ACS Environ. Au* **2021**, *I*, 18. (24) Hrudey, S. E.; Conant, B. The Devil Is in the Details: Emerging Insights on the Relevance of Wastewater Surveillance for SARS-CoV-2 to Public Health. *J. Water Health* **2022**, 20 (1), 246–270.
- (25) Ciesielski, M.; Blackwood, D.; Clerkin, T.; Gonzalez, R.; Thompson, H.; Larson, A.; Noble, R. Assessing Sensitivity and Reproducibility of RT-DdPCR and RT-QPCR for the Quantification of SARS-CoV-2 in Wastewater. *J. Virol. Methods* **2021**, 297, 114230. (26) Hamouda, M.; Mustafa, F.; Maraqa, M.; Rizvi, T.; Aly Hassan, A. Wastewater Surveillance for SARS-CoV-2: Lessons Learnt from
- Recent Studies to Define Future Applications. *Sci. Total Environ.* **2021**, 759, 143493. (27) Cohen, A.; Grubb, C. Virginia Tech SARS-CoV-2 Wastewater Surveillance & COVID-19 Epidemiology Initiative: Statistical Analysis
- Plan. Open Science Framework; 2021; https://osf.io/f4eax/. (28) Ahmed, W.; Bertsch, P. M.; Bivins, A.; Bibby, K.; Farkas, K.; Gathercole, A.; Haramoto, E.; Gyawali, P.; Korajkic, A.; McMinn, B. R.; Mueller, J. F.; Simpson, S. L.; Smith, W. J. M.; Symonds, E. M.; Thomas, K. V.; Verhagen, R.; Kitajima, M. Comparison of Virus Concentration Methods for the RT-QPCR-Based Recovery of Murine Hepatitis Virus, a Surrogate for SARS-CoV-2 from Untreated Wastewater. Sci. Total Environ. 2020, 739, 139960.
- (29) Ceci, A.; Muñoz-Ballester, C.; Tegge, A. N.; Brown, K. L.; Umans, R. A.; Michel, F. M.; Patel, D.; Tewari, B.; Martin, J.; Alcoreza, O.; Maynard, T.; Martinez-Martinez, D.; Bordwine, P.; Bissell, N.; Friedlander, M. J.; Sontheimer, H.; Finkielstein, C. V. Development and Implementation of a Scalable and Versatile Test for COVID-19 Diagnostics in Rural Communities. *Nat. Commun.* 2021, 12 (1), 4400–4400.
- (30) Gonzalez, R.; Larson, A.; Thompson, H.; Carter, E.; Cassi, X. F. Redesigning SARS-CoV-2 Clinical RT-QPCR Assays for Wastewater RT-DdPCR. *medRxiv* **2021**, 2021.03.02.21252754; DOI: 10.1101/2021.03.02.21252754.
- (31) Bibby, K.; Bivins, A.; Wu, Z.; North, D. Making Waves: Plausible Lead Time for Wastewater Based Epidemiology as an Early Warning System for COVID-19. *Water Res.* **2021**, 202, 117438.
- (32) Olesen, S. W.; Imakaev, M.; Duvallet, C. Making Waves: Defining the Lead Time of Wastewater-Based Epidemiology for COVID-19. *Water Res.* **2021**, 202, 117433.

- (33) Galani, A.; Aalizadeh, R.; Kostakis, M.; Markou, A.; Alygizakis, N.; Lytras, T.; Adamopoulos, P. G.; Peccia, J.; Thompson, D. C.; Kontou, A.; Karagiannidis, A.; Lianidou, E. S.; Avgeris, M.; Paraskevis, D.; Tsiodras, S.; Scorilas, A.; Vasiliou, V.; Dimopoulos, M.-A.; Thomaidis, N. S. SARS-CoV-2 Wastewater Surveillance Data Can Predict Hospitalizations and ICU Admissions. *Sci. Total Environ.* 2022, 804, 150151.
- (34) Corchis-Scott, R.; Geng, Q.; Seth, R.; Ray, R.; Beg, M.; Biswas, N.; Charron, L.; Drouillard, K. D.; D'Souza, R.; Heath, D. D.; Houser, C.; Lawal, F.; McGinlay, J.; Menard, S. L.; Porter, L. A.; Rawlings, D.; Scholl, M. L.; Siu, K. W. M.; Tong, Y.; Weisener, C. G.; Wilhelm, S. W.; McKay, R. M. L. Averting an Outbreak of SARS-CoV-2 in a University Residence Hall through Wastewater Surveillance. *Microbiol. Spectr.* 2021, 9 (2), No. e00792-21.
- (35) Juel, M. A. I.; Stark, N.; Nicolosi, B.; Lontai, J.; Lambirth, K.; Schlueter, J.; Gibas, C.; Munir, M. Performance Evaluation of Virus Concentration Methods for Implementing SARS-CoV-2 Wastewater Based Epidemiology Emphasizing Quick Data Turnaround. *Sci. Total Environ.* **2021**, *801*, 149656.
- (36) Karthikeyan, S.; Nguyen, A.; McDonald, D.; Zong, Y.; Ronquillo, N.; Ren, J.; Zou, J.; Farmer, S.; Humphrey, G.; Henderson, D.; Javidi, T.; Messer, K.; Anderson, C.; Schooley, R.; Martin, N. K.; Knight, R. Rapid, Large-Scale Wastewater Surveillance and Automated Reporting System Enable Early Detection of Nearly 85% of COVID-19 Cases on a University Campus. *mSystems* **2021**, *6* (4), No. e00793-21.
- (37) Reeves, K.; Liebig, J.; Feula, A.; Saldi, T.; Lasda, E.; Johnson, W.; Lilienfeld, J.; Maggi, J.; Pulley, K.; Wilkerson, P. J.; Real, B.; Zak, G.; Davis, J.; Fink, M.; Gonzales, P.; Hager, C.; Ozeroff, C.; Tat, K.; Alkire, M.; Butler, C.; Coe, E.; Darby, J.; Freeman, N.; Heuer, H.; Jones, J. R.; Karr, M.; Key, S.; Maxwell, K.; Nelson, L.; Saldana, E.; Shea, R.; Salveson, L.; Tomlinson, K.; Vargas-Barriga, J.; Vigil, B.; Brisson, G.; Parker, R.; Leinwand, L. A.; Bjorkman, K.; Mansfeldt, C. High-Resolution within-Sewer SARS-CoV-2 Surveillance Facilitates Informed Intervention. *Water Res.* 2021, 204, 117613.
- (38) Schmitz, B. W.; Innes, G. K.; Prasek, S. M.; Betancourt, W. Q.; Stark, E. R.; Foster, A. R.; Abraham, A. G.; Gerba, C. P.; Pepper, I. L. Enumerating Asymptomatic COVID-19 Cases and Estimating SARS-CoV-2 Fecal Shedding Rates via Wastewater-Based Epidemiology. *Sci. Total Environ.* **2021**, *801*, 149794.
- (39) Scott, L. C.; Aubee, A.; Babahaji, L.; Vigil, K.; Tims, S.; Aw, T. G. Targeted Wastewater Surveillance of SARS-CoV-2 on a University Campus for COVID-19 Outbreak Detection and Mitigation. *Environ. Res.* **2021**, *200*, 111374.